JOC Article
pubs.acs.org/joc

Effect of the Electron Donor/Acceptor Orientation on the Fluorescence Transduction Efficiency of the d-PET Effect of Carbazole-Based Fluorescent Boronic Acid Sensors

Xin Zhang,[†] Yubo Wu,[†] Shaomin Ji,[†] Huimin Guo,[‡] Peng Song,[§] Keli Han,[§,‡] Wenting Wu, Wanhua Wu, Tony D. James,[∥] and Jianzhang Zhao*,[†]

[†]*State Key Laboratory of Fine Chemicals, and* [‡]*Department of Chemistry, School of Chemical Engineering, Dalian University of Technology, Dalian 116012, P. R. China,* [§]*State Key Laboratory of Molecular Reaction Dynamics, Dalian Institute of Chemical Physics, Chinese Academy of Sciences, 457 Zhongshan Road, Dalian 116023, P. R. China, and* [∥]*Department of Chemistry, University of Bath, Bath BA2 7AY, U.K.*

zhaojzh@dlut.edu.cn

Received January 24, 2010

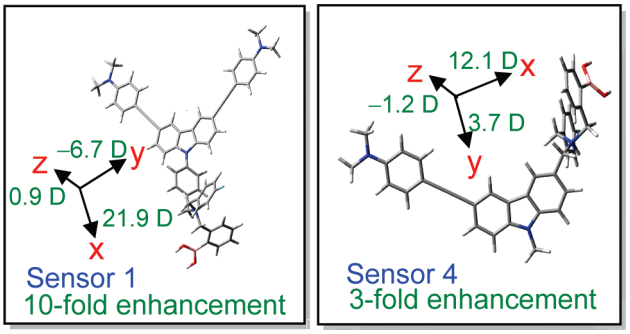

We have synthesized three new carbazole-based fluorescent boronic acid sensors to investigate the fluorescence transduction efficiency of the novel d-PET effect, in which the fluorophore acts as the electron donor and the protonated amine/boronic acid group as the electron acceptor of the photoinduced electron transfer process (PET). Aryl ethynyl groups are attached at the 3,6-position of carbazole (aryl = 4-dimethylaminophenyl for sensor **1** or phenyl for sensor **2**). Sensor **3** is without 3,6-substitutions. The phenylboronic acid moiety is attached at the 9-position (*N*-atom) of the carbazole in these sensors. We found that **1** and **3** are d-PET sensors (fluorophore as the electron *d*onor, supported by DFT/TDDFT calculations), which show diminished emission at acidic pH but intensified emission at neutral/basic pH, which is in stark contrast to the normal a-PET (fluorophore as the electron *a*cceptor) sensors, e.g., **2**, which shows intensified emission at acidic pH but diminished emission at neutral pH. The fluorescence modulation efficiency of the d-PET effect of the new sensors, i.e., the emission intensity enhancement upon switching from acidic pH to neutral pH, is up to 10-fold, which is greatly improved compared to our previous d-PET sensors (ca. 3-fold). The efficient d-PET effect of the new sensors is attributed to the proper orientation of the electron donor/acceptor; i.e., the dipole moment and the transition moment (the direction of PET) of the new sensors are oriented in the same direction, and the dipole moment values of the new sensors along the vector direction of the PET are larger than that of the reported d-PET sensors. Selective recognition of α-hydroxyl carboxylic acids, such as tartaric acid, was achieved with the d-PET sensors, and a novel fluorescence transduction profile of enhancement/diminishment for chemoselectivity was observed. Herein we propose that the orientation of the electron donor/acceptor may significantly affect the fluorescence modulation efficiency of the PET effect; this discovery will be important for the future design of PET sensors with improved fluorescence transduction efficiencies.

1. Introduction

Recently, fluorescent molecular sensors have attracted much attention due to their versatile applications in chemical, biological, and environmental science.[1−14] Usually, the structure of the molecular sensors can be divided into three modular parts, i.e., the binding unit, the fluorophore, and the linker between the two parts.[2,3,5] Much effort has been taken to develop these three modular parts, e.g., new binding units

Published on Web 03/22/2010 DOI: 10.1021/jo100119y

to achieve better selectivity and sensitivity toward analytes, such as crown ether for metal cations, di(2-picolyl)amine (DPA) for Zn^{2+} and Cd^{2+}, etc.[15−18] Recently, new fluorophores, such as BODIPY and merocyanine dyes, have been developed to improve the photophysical properties of the fluorescent molecular sensors, such as the emission wavelength and the fluorescence quantum yields.[19−27] The linker between the binding unit and the fluorophore is also found to be important for molecular sensing.[3] However, besides the aforementioned three modular parts of a sensor molecule, there exists the fourth important factor, i.e., the sensing mechanism, or the mechanism of signal transduction upon molecular recognition (analyte binding), which is also essential for a successful sensor design since the sensing mechanism can also dictate the selectivity and sensitivity of fluorescent molecular sensors.[27−32] However, in contrast to the rigorous investigations carried out on the binding units and the fluorophores, reports on new fluorescence-sensing mechanisms are very limited.[3,7,16,33−36] Most popular sensing mechanisms include photoinduced electron transfer (PET), intramolecular charge transfer (ICT), or the caged fluorophores strategies.[16,31,37,38] However, it is still a major challenge to develop new fluorescence sensing mechanisms, with which the intrinsic drawbacks of the traditional sensing mechanisms can be addressed. For example, the protonation of the fluorophore non-conjugated *N* atom of the conventional a-PET fluorescent sensors at acidic pH may impart significant interference on the fluorescent sensing, in which the fluorophore acts as the electron acceptor of the PET process.[39,40] In order to reduce the background emission of the a-PET sensors, new sensing mechanisms have to be developed.

We have been interested for a number of years in boronic acid fluorescent sensors and developing new fluorescence-sensing mechanisms, such as d-PET effect (fluorophore as the electron donor of the PET), which demonstrates reversed emission intensity−pH profile compared to the normal a-PET sensors.[38−44] Boronic acid sensors are unique in that they are effective in aqueous media due to the covalent nature of the interaction of the boronic acid group with the polyhydroxyl analytes, such as glucose, tartaric acid, etc.[3,45−59] Boronic acid sensors are usually based on a-PET sensing mechanism,[3,7] in which the fluorophore acts as the electron acceptor and the nonfluorophore-conjugated *N* atom as the electron donor of the PET process.[7] Thus, these normal a-PET sensors show strong background emission at acidic pH due to the protonation of the *N* atom, and thereafter, the inhibition of the PET process, as a result the fluorescence emission will be intensified. It should be pointed out that fluorescence signal transduction of the a-PET sensors upon binding with analytes employs the same inhibition of the PET process; thus, protonation of the sensor at acidic pH will impart significant interference on the fluorescent recognition of analytes with the normal a-PET sensors.[7,39,40] However, with boronic acid sensors, some analytes require acidic pH to achieve strong binding, and as such, the interference of protonation of the amine on the

(1) Kim, S. K.; Lee, D. H.; Hong, J.; Yoon, J. *Acc. Chem. Res.* **2009**, *42*, 23–31.
(2) Wright, A. T.; Anslyn, E. V. *Chem. Soc. Rev.* **2006**, *35*, 14–28.
(3) James, T. D. *Top. Curr. Chem.* **2007**, *277*, 107–152.
(4) Davis, A. P. *Org. Biomol. Chem.* **2009**, *7*, 3629–3638.
(5) Pu, L. *Chem. Rev.* **1998**, *98*, 2405–2494.
(6) Pu, L. *Chem. Rev.* **2004**, *104*, 1687–1716.
(7) De Silva, A. P.; Gunaratne, H. Q. N.; Gunnlaugsson, T.; Huxley, A. J. M.; McCoy, C. P.; Rademacher, J. T.; Rice, T. E. *Chem. Rev.* **1997**, *97*, 1515–1566.
(8) Dos Santos, C. M. G.; Harte, A. J.; Quinn, S. J.; Gunnlaugsson, T. *Coord. Chem. Rev.* **2008**, *252*, 2512–2527.
(9) Oshovsky, G. V.; Reinhoudt, D. N.; Verboom, W. *Angew. Chem., Int. Ed.* **2007**, *46*, 2366–2393.
(10) Cametti, M.; Rissanen, K. *Chem. Commun.* **2009**, 2809–2829.
(11) Caltagirone, C.; Gale, P. A. *Chem. Soc. Rev.* **2009**, *38*, 520–563.
(12) Stibor, I.; Zlatuskova, P. *Top. Curr. Chem.* **2005**, *255*, 31–63.
(13) Suksai, C.; Tuntulani, T. *Top. Curr. Chem.* **2005**, *255*, 163–198.
(14) Wolf, C.; Mei, X. *J. Am. Chem. Soc.* **2003**, *125*, 10651–10658.
(15) Ito, H.; Matsuoka, M.; Ueda, Y.; Takuma, M.; Kudo, Y.; Iguchi, K. *Tetrahedron* **2009**, *65*, 4235–4238.
(16) Yang, Y.; Lee, S.; Tae, J. *Org. Lett.* **2009**, *11*, 5610–5613.
(17) Dodani, S. C.; He, Q.; Chang, C. J. *J. Am. Chem. Soc.* **2009**, *131*, 18020–18021.
(18) Li, H.; Li, Y.; Dang, Y.; Ma, L.; Wu, Y.; Hou, G.; Wu, L. *Chem. Commun.* **2009**, 4453–4455.
(19) Ulrich, G.; Ziessel, R.; Harriman, A.; Ulrich, G.; Ziessel, R.; Harriman, A. *Angew. Chem., Int. Ed.* **2008**, *47*, 1184–1201.
(20) Wu, L.; Kevin, B. *Chem. Commun.* **2008**, 4933–4935.
(21) Yogo, T.; Urano, Y.; Ishitsuka, Y.; Maniwa, F.; Nagano, T. *J. Am. Chem. Soc.* **2005**, *127*, 12162–12163.
(22) Lee, J.; Kang, N.; Kim, Y. K.; Samanta, A.; Feng, S.; Kim, H. K.; Vendrell, M.; Park, J. H.; Chang, Y. *J. Am. Chem. Soc.* **2009**, *131*, 10077–10082.
(23) Cheng, T.; Xu, Y.; Zhang, S.; Zhu, W.; Qian, X.; Duan, L. *J. Am. Chem. Soc.* **2008**, *130*, 16160–16161.
(24) Mohr, G. J. *Chem.—Eur. J.* **2009**, *15*, 418–423.
(25) Zhou, Y.; Xiao, Y.; Chi, S.; Qian, X. *Org. Lett.* **2008**, *10*, 633–636.
(26) Peng, X.; Song, F.; Lu, E.; Wang, Y.; Zhou, W.; Fan, J.; Gao, Y. *J. Am. Chem. Soc.* **2005**, *127*, 4170–4171.
(27) Kundu, K.; Knight, S. F.; Willett, N.; Lee, S.; Taylor, W. R.; Murthy, N. *Angew. Chem., Int. Ed.* **2009**, *48*, 299–303.
(28) Zhang, X.; Xiao, Y.; Qian, X. *Angew. Chem., Int. Ed.* **2008**, *47*, 8025–8029.
(29) Sun, Z.; Liu, F.; Chen, Y.; Tam, P. K. H.; Yang, D. *Org. Lett.* **2008**, *10*, 2171–2174.
(30) Srikun, D.; Miller, E. W.; Domaille, D. W.; Chang, C. J. *J. Am. Chem. Soc.* **2008**, *130*, 4596–4597.
(31) Miller, E. W.; Albers, A. E.; Pralle, A.; Isacoff, E. Y.; Chang, C. J. *J. Am. Chem. Soc.* **2005**, *127*, 16652–16659.
(32) Ji, S.; Yang, J.; Yang, Q.; Liu, S.; Chen, M.; Zhao, J. *J. Org. Chem.* **2009**, *74*, 4855–4865.
(33) Jou, M. J.; Chen, X.; Swamy, K. M. K.; Kim, H. N.; Kim, H.; Lee, S.; Yoon, J. *Chem. Commun.* **2009**, 7218–7220.
(34) James, T. D.; Shinkai, S. *Top. Curr. Chem.* **2002**, *218*, 159–200.
(35) Fujita, N.; Shinkai, S.; James, T. D. *Chem. Asian J.* **2008**, *3*, 1076–1091.
(36) Mohr, G. J. *Chem.—Eur. J.* **2004**, *10*, 1082–1090.
(37) Han, F.; Chi, L.; Liang, X.; Ji, S.; Liu, S.; Zhou, F.; Wu, Y.; Han, K.; Zhao, J.; James, T. D. *J. Org. Chem.* **2009**, *74*, 1333–1336.
(38) Zhang, X.; Chi, L.; Ji, S.; Wu, Y.; Song, P.; Han, K.; Guo, H.; James, T. D.; Zhao, J. *J. Am. Chem. Soc.* **2009**, *131*, 17452–17463.
(39) Zhao, J.; Fyles, T. M.; James, T. D. *Angew. Chem. Int. Ed.* **2004**, *43*, 3461–3464
(40) Zhao, J.; Davidson, M. G.; Mahon, M. F.; Kociok-Kohn, G.; James, T. D. *J. Am. Chem. Soc.* **2004**, *126*, 16179–16186.
(41) Zhao, J.; James, T. D. *J. Mater. Chem.* **2005**, *15*, 2896–2901.
(42) Zhao, J.; James, T. D. *Chem. Commun.* **2005**, 1889–1891.
(43) Liang, X.; James, T. D.; Zhao, J. *Tetrahedron* **2008**, *64*, 1309–1315.
(44) Chi, L.; Zhao, J.; James, T. D. *J. Org. Chem.* **2008**, *73*, 4684–4687.
(45) Lavigne, J. J.; Anslyn, E. V. *Angew. Chem., Int. Ed.* **1999**, *38*, 3666–3669.
(46) Zhang, L.; Kerszulis, J. A.; Clark, R. J.; Ye, T.; Zhu, L. *Chem. Commun.* **2009**, 2151–2153.
(47) Wang, J.; Jin, S.; Akay, S.; Wang, B. *Eur. J. Org. Chem.* **2007**, 2091–2099.
(48) Jin, S.; Wang, J.; Li, M.; Wang, B. *Chem.—Eur. J.* **2008**, *14*, 2795–2804.
(49) Nonaka, A.; Horie, S.; James, T. D.; Kubo, Y. *Org. Biomol. Chem.* **2008**, *6*, 3621–3625.
(50) Scrafton, D. K.; Taylor, J. E.; Mahon, M. F.; Fossey, J. S.; James, T. D. *J. Org. Chem.* **2008**, *73*, 2871–2874.
(51) Bromba, C.; Carrie, P.; Chui, J. K. W.; Fyles, T. M. *Supramol. Chem.* **2009**, *21*, 81–88.
(52) Halo, T. L.; Appelbaum, J.; Hobert, E. M.; Balkin, D. M.; Schepartz, A. *J. Am. Chem. Soc.* **2009**, *131*, 438–439.
(53) Levonis, S. M.; Kiefel, M. J.; Houston, T. A. *Chem. Commun.* **2009**, 2278–2280.
(54) Trupp, S.; Schweitzer, A.; Mohr, G. J. *Org. Biomol. Chem.* **2006**, *4*, 2965–2968.
(55) He, M.; Johnson, R. J.; Escobedo, J. O.; Beck, P. A.; Kim, K. K.; Luce, N. N.; St. Davis, C. J.; Lewis, P. T.; Fronczek, F. R.; Melancon, B. J.; Mrse, A. A.; Treleaven, W. D.; Strongin, R. M. *J. Am. Chem. Soc.* **2002**, *124*, 5000–5009.
(56) Musto, C. J.; Lim, S. H.; Suslick, K. S. *Anal. Chem.* **2009**, *81*, 6526–6533.
(57) Kim, K. T.; Cornelissen, J. J. L. M.; Nolte, R. J. M.; van Hest, J. C. M. *J. Am. Chem. Soc.* **2009**, *131*, 13908–13909.
(58) Tan, W.; Zhang, D.; Zhu, D. *Bioorg. Med. Chem. Lett.* **2007**, *17*, 2629–2633.
(59) Zhang, J.; Geddes, C. D.; Lakowicz, J. R. *Anal. Biochem.* **2004**, *332*, 253–260.

fluorescence is significant.[39,40] The normal a-PET sensors give small fluorescence response at acid pH.[3,7,39,40,47] Therefore, the molecular sensors based on the traditional a-PET mechanisms cannot address the interference of protonation at acidic pH.

Recently, we have found that carbazole-based boronic acid sensors show the novel d-PET effect.[37,38,60,61] This reversed PET will result in quenched fluorescence at acidic pH; thus, these d-PET sensors give weak background emission at acidic pH.[37,38] Binding with analytes will suppress this quenching process, due to the strengthened B−N interaction (the ET from the fluorophore to the protonated amine/boronic acid moiety is inhibited), through either a direct B−N interaction or intramolecular hydrogen-bonded (solvent molecule inserted) zwitterionic structure,[40,46,62,63] and fluorescence enhancement was observed. This fluorescence signal transduction is in contrast to the normal PET effect, i.e., the a-PET effect, in which the fluorophore acts as the electron acceptor and the nonconjugated *N* atom as the electron donor of the PET. This novel d-PET effect may prove useful for design of new PET sensors to address the challenges imposed by the traditional PET mechanism, such as poor fluorescence response of the a-PET sensors at acid pH.[39−41]

However, as the d-PET sensors are rarely reported,[37,38,60,61,64] the current understanding of the d-PET effect is in its infancy, let alone rational design of d-PET sensors. As a preliminary exploration, we have demonstrated that DFT/TDDFT calculations can be used for rational design of carbazole-based d-PET boronic acid sensors.[38] However, the performance of these reported d-PET boronic acid sensors is not satisfying.[37,38] For example, the fluorescence modulation efficiency is very low; e.g., with the pH switched from acidic to neutral, the fluorescence intensity enhancement is only 0.25-fold (sensor **6**, Scheme 1)[37] or 3-fold (sensor **4**, Scheme 1).[38] These values are much lower compared to the fluorescence transduction efficiency of the traditional a-PET sensors,[40] which show several folds of emission variation. Thus, we set out to prepare new d-PET sensors, to investigate the structure−performance relationship, and finally, to improve the d-PET efficiencies.

Herein, we synthesized new carbazole-based boronic acid sensors. Arylethynyl groups were introduced on the 3,6-position of the carbazole, and the boronic acid group is attached at the 9-position of the carbazole fluorophore. The arylethynyl appendents were designed as either electron-donating (dimethylamino group, sensor **1**) or for extension of the π-conjugation framework (phenylethynyl, sensor **2**). A model sensor without arylethynyl substitution was also prepared (sensor **3**). The structures of these sensors are fundamentally different from the previous d-PET sensors reported by us.[37,38] First, the orientation of the electron donor/acceptor in these sensors is different and the alignment of the donor/acceptor of the new sensors are more appropriate for the potential PET process because the dipole moment and the transition moment (or the vector direction of the PET effect) of the sensors are oriented in the same direction (Scheme 1 and Figure 3). For the previously reported sensors, however, the orientation of the electron donor/acceptor is not ideal for the PET process. This was demonstrated by the dipole moment values of the sensor along the PET direction. Thus, more efficient PET and higher fluorescence transduction efficiency can be expected for the new sensors. Second, the nonconjugated *N* atom of the new sensors, which acts as the switch of the fluorescence of PET sensors,[3,7,34] is not in immediate proximity to the fluorophore. We expect this increased *N*-fluorophore distance may significantly diminish the PET effect because it is known that the PET efficiency is strongly dependent on the distance between the nonconjugated *N* atom and the fluorophore; in order to achieve efficient PET effect, usually the linker is as short as a methylene group ($-CH_2-$).[3,7,39,40] Interestingly, the new sensors still demonstrated high fluorescence transduction efficiencies even with the large distance between fluorophore and the *N* atom. For example, as high as 10-fold of fluorescence emission intensity enhancement was observed for sensor **1** on switching the pH from acidic to neutral/basic. Furthermore, we found that the boronic acid moiety plays a significant role in the d-PET effect. For example, amine **11** (precursor of sensor **3**) shows the normal a-PET effect, whereas the boronic acid sensor **3** shows the d-PET effect. Thus, we propose that the boronic acid group is an electron acceptor, and it facilitates the occurrence of the d-PET effect of sensor **3**. Third, we found that the phenylethynyl moiety is electron-deficient and may diminish the d-PET effect. For example, sensor **3** is a d-PET sensor, but sensor **2**, with the phenylethynyl group attached at the 3,6-position of the carbazole, is an a-PET sensor. We have demonstrated that the d-PET effect of sensor **1** can be rationalized with DFT/TDDFT calculations. Selective recognition toward α-hydroxyl acids, such as tartaric acid and mandelic acid, was achieved with the new boronic acid sensors. A good signal transduction profile was also observed for the sensors. For example, fluorescence enhancement/diminishment was observed for sensor **3** upon binding of tartaric acid and mandelic acid at pH 5.0. We believe our study on the d-PET effect and the discovery that the orientation of the electron donor/acceptor on the fluorescence transduction efficiency of the PET effect will be very useful in future sensor design in order to optimize the signal transduction of PET sensors and to achieve OFF−ON modulation with enhanced sensitivity.[3,65−72]

2. Results and Discussion

2.1. Design and Synthesis of the Carbazole-Based Boronic Acid Sensors. Previously, we reported the d-PET effect of the

(60) Ueno, T.; Urano, Y.; Setsukinai, K.; Takakusa, H.; Kojima, H.; Kikuchi, K.; Ohkubo, K.; Fukuzumi, S.; Nagano, T. *J. Am. Chem. Soc.* **2004**, *126*, 14079–14085.
(61) Matsumoto, T.; Urano, Y.; Shoda, T.; Kojima, H.; Nagano, T. *Org. Lett.* **2007**, *9*, 3375–3377.
(62) Zhu, L.; Shabbir, S. H.; Gray, M.; Lynch, V. M.; Sorey, S.; Anslyn, E. V. *J. Am. Chem. Soc.* **2006**, *128*, 1222–1232.
(63) Collins, B. E.; Sorey, S.; Hargrove, A. E.; Shabbir, S. H.; Lynch, V. M.; Anslyn, E. V. *J. Org. Chem.* **2009**, *74*, 4055–4060.
(64) Mineno, T.; Ueno, T.; Urano, Y.; Kojima, H.; Nagano, T. *Org. Lett.* **2006**, *8*, 5963–5966.
(65) Zhou, Y.; Wang, F.; Kim, Y.; Kim, S.; Yoon, J. *Org. Lett.* **2009**, *11*, 4442–4445.
(66) Gao, X.; Zhang, Y.; Wang, B. *Org. Lett.* **2003**, *5*, 4615–4618.
(67) Zhao, Y.; Zhang, X.; Han, Z.; Xiao, L.; Li, C.; Jean, L.; Sheen, G.; Yu, R. *Anal. Chem.* **2009**, *81*, 7022–7030.
(68) Cody, J.; Manual, S.; Yang, L.; Farina, C. J. *J. Am. Chem. Soc.* **2008**, *130*, 13023–13032.
(69) de Silva, S. A.; Look, K. C.; Amorally, B.; Parthian, S. L.; Nyakirang'ani, M.; Dharmasena, M.; Demarais, S.; Dorcley, B.; Pullay, P.; Salih, Y. A. *J. Mater. Chem.* **2005**, *15*, 2791–2795.
(70) Wu, J.; Hwang, I.; Kim, K. S.; Kim, J. S. *Org. Lett.* **2007**, *9*, 907–710.
(71) Kenmoku, S.; Urano, Y.; Kojima, H.; Nagano, T. *J. Am. Chem. Soc.* **2007**, *129*, 7313–7318.
(72) Chang, M. C. Y.; Pralle, A.; Isacoff, E. Y.; Chang, C. J. *J. Am. Chem. Soc.* **2004**, *126*, 15392–15393.

SCHEME 1. Synthesis of the 3,6-Aryldiethynyl-Substituted Boronic Acid Sensors 1 and 2 and *N*-Substituted Boronic Acid Sensor 3[a]

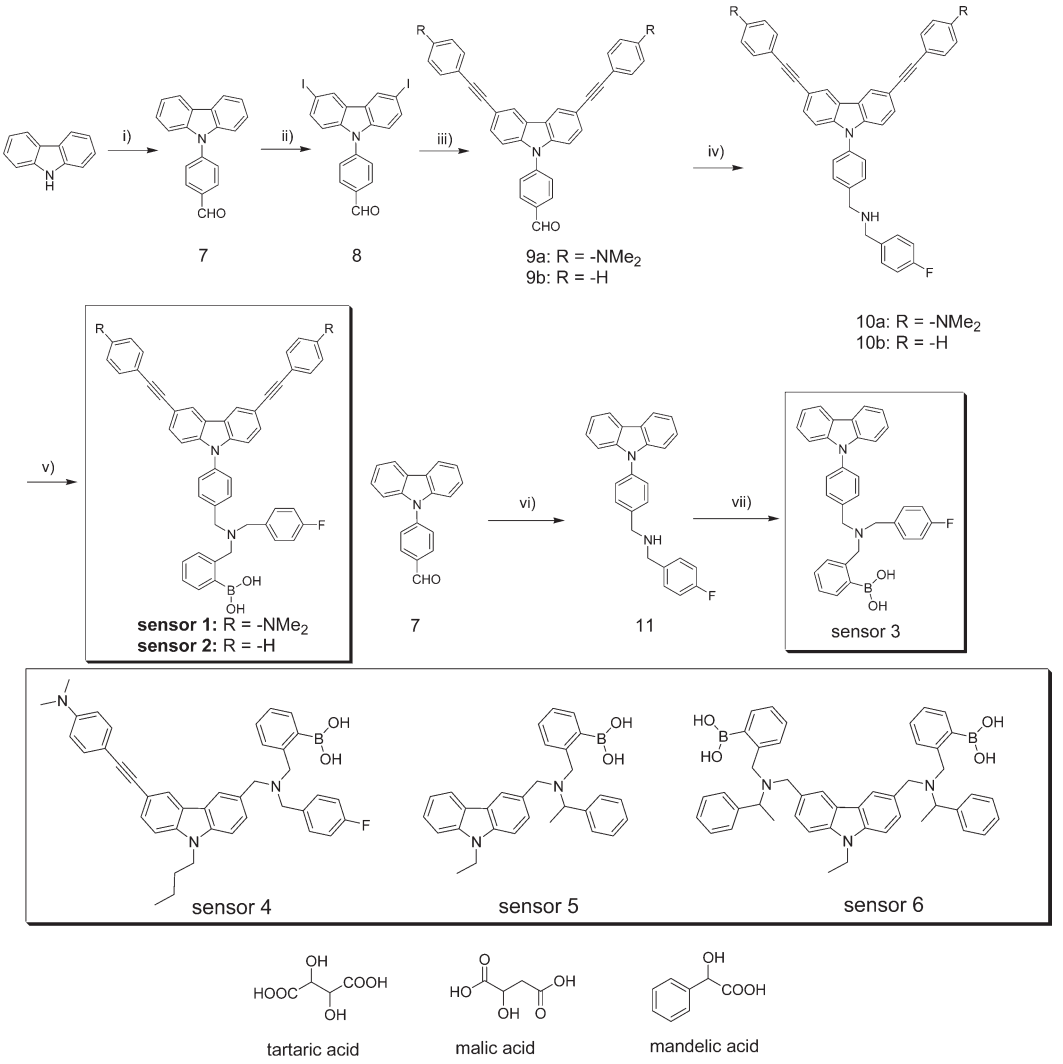

[a]The reported d-PET boronic acid sensors **4**−**6**, as well as the structures of the analytes used in the binding study, are also presented: (i) 4-fluorobenzaldehyde, hexadecyltrimethylammonium bromide, K_2CO_3, DMSO, 100 °C, 72 h, 35.0%; (ii) KI, KIO_3, CH_3COOH, 80 °C, 5 h, 76.0%; (iii) $Pd(PPh_3)_4$, CuI, NEt_3, 4-ethynyl-*N*,*N*-dimethylaniline or ethynylbenzene, argon atmosphere, 60 °C, 8 h, 33.0−56.0%; (iv) ethanol, THF, 4-fluorobenzylamine, reflux, 6 h, then methanol, THF, $NaBH_4$, room temperature, 15 min; (v) dichloromethane, K_2CO_3, 2-(2-bromomethylphenyl)-1,3,2-dioxaborinane, room temperature 12 h, 37.0%−44.0%; (vi) ethanol, THF, 4-fluorobenzylamine, reflux, 6 h, then methanol, THF, $NaBH_4$, room temperature, 15 min; (vii) dichloromethane, K_2CO_3, 2-(2-bromomethylphenyl)-1,3,2-dioxaborinane, room temperature, 12 h, 39.0%.

carbazole based boronic acid sensors (**4**−**6**, Scheme 1).[37,38] The structure of sensors **4** and **6** is based on 3,6-substituted carbazole fluorophore, whereas sensor **5** was based on 3-subsituted carbazole. In these sensors, the alkyl *N* atom (nonconjugated with the fluorophore), which is the switch of the fluorescence,[7] is close to the fluorophore (with a $-CH_2-$ linker); thus, these sensors are the traditional PET type of sensor.[3,7] For the new sensors **1**−**3**, however, the phenylboronic acid moiety is attached to the carbazole core at the 9-position (*N*-atom); thus, the distance between the alkyl *N* atom and the fluorophore is much larger than the sensors **4**−**6**. Our DFT calculation shows that the phenyl group directly attached to the carbazole *N*-atom is not coplanar with the carbazole core; thus, it is not involved in the π-conjugation framework. We used aryl ethynyl substituents at the 3,6-positions of the carbazole core to modulate the electron-donating/withdrawal property of the fluorophore and, hence, tune the PET effect. The structures of these new sensors are fundamentally different from those of the reported sensors **4** and **5** with regard to the orientation of the electron donor (carbazole) and the electron acceptor; furthermore, the nonconjugated *N* atom is not in immediate proximity to the fluorophore; therefore, it will be interesting to investigate the PET efficiency of the new sensors because it is known that the PET effect is strongly dependent on the distance between the *N* atom and the fluorophore.[7]

The new sensors belong to the Wulff type of boronic acid sensors, in which the alkyl *N* atom close to the boronic acid group strengthens the B−N interaction, thus stabilizing the sensor−analyte binding complex.[3] The 4-formylphenyl moiety is introduced to the 9-position of the carbazole by reaction of carbazole with 4-fluorobenzaldehyde. Then the intermediate **7** was iodized. The palladium-catalyzed Sonogashira coupling reaction was used to extend the π-conjugation

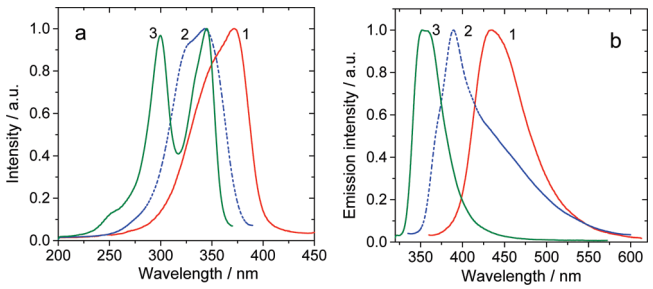

FIGURE 1. Normalized fluorescence (a) excitation and (b) emission spectra of the sensors **1**−**3**. For sensor **1**: λ_{ex}, 372 nm; λ_{em}, 435 nm. For sensor **2**: λ_{ex}, 343 nm; λ_{em}, 390 nm. For sensor **3**: λ_{ex}, 345 nm; λ_{em}, 356 nm. 1.0×10^{-6} mol dm^{-3} of sensors in 0.05 mol dm^{-3} NaCl ionic buffer (52.1% methanol in water). pH 7.4, 25 °C.

of the carbazole core to optimize the emission property (such as to extend the emission wavelength) and to tune the electron-withdrawal/donating property of the fluorophore. Herein we used the C≡C triple bond as the conjugation bridge, instead of the C=C double bonds. It is known the super fast cis/trans isomerization of the C=C double bonds in the excited state may severely quench the fluorescence.[73,74] With reductive amination and introduction of the boronic acid moiety, sensors **1** and **2** were obtained. As a model sensor, **3** was also prepared without 3,6-substitution. All of the sensors were obtained with satisfying yields.

2.2. Fluorescence Emission of the Sensors and the a-PET/d-PET Effects. The fluorescence spectra of the sensors were measured (Figure 1). For the model sensor **3**, which is devoid of the arylethynyl fragments at the 3,6-position of the fluorophore, excitation and emission wavelength at the blue end of the spectrum were observed. The emission wavelength is slightly blue-shifted compared to the reported sensor **5**.[37] We propose that the electronic structure, or the π-conjugation framework of carbazole, is not perturbed with *N*-substitution. For the sensors **1** and **2**, however, drastically different excitation/emission profiles were observed. For example, the excitation spectrum is a broad, without any fine structures, and the emission wavelength is red-shifted by up to 100 nm compared to the model sensor **3**. These emission profiles indicate that the electronic structure of sensors **1** and **2** have been significantly altered when compared to that of sensors **3** and **5**, which is due to the efficient π-conjugation effect through the C≡C triple bonds.

In order to study the PET effect of the sensors, the emission intensity−pH profiles of the sensors and the respective amine precursors were measured (Figure 2). The amine **10a** shows diminished emission at acidic pH. At neutral and basic pH, however, the emission intensity is enhanced. This is the typical d-PET signal transduction.[37,38] The apparent pK_a of the amine **10a** is 6.35 ± 0.09 ($r^2 = 0.97$). The emission intensity−pH profile of the sensor **1** was then measured and d-PET effect was also observed. The fluorescence enhancement upon switching the pH from acidic to neutral is as high as 10-fold. Interestingly, a much smaller pK_a of 3.18 ± 0.11 ($r^2 = 0.92$) was observed. We attribute the variation of the pK_a to the B−N interaction in the boronic acid sensor, either directly or through an intramolecular hydrogen bond.[40,46,62,63]

The emission intensity−pH profile of sensor **2** was also measured (Figure 2b). Interestingly, both the amine precursor **10b** and **2** show the normal a-PET effect; i.e. the emission is intensified at acidic pH but diminished at neutral and basic pH.[3,39−43] Comparison of the molecular structure and spectral properties between the amine **10a**/**10b** and **1**/**2** indicates that an electron-donating group (dimethylamino) on the 4-position of the phenylethynyl group is essential for the observation of the d-PET effect. Based on the results of **3** (see below), we deduce that the phenylethynyl group is electron-deficient. This result may prove helpful for future design of ethynylated carbazole-based PET sensors.

The amine **11** and sensor **3** were also investigated (Figure 2c). Interestingly, normal a-PET effect was observed for amine **11**, with pK_a of 7.90 ± 0.03 ($r^2 = 0.99$). For **3**, however, typical d-PET effect was observed, with pK_a value of 4.76 ± 0.04 ($r^2 = 0.99$). This result clearly demonstrates the important role of the boronic acid group in the realization of the d-PET effect. The boronic acid group is an electron-deficient center; therefore, the d-PET effect can be facilitated.

The typical fluorescence emission spectra of the sensors on switching from acidic to basic pH are presented in Figure 2d−f. For the **1** and **3**, fluorescence emission diminishment was observed when the pH was switched from neutral/basic range to acidic pH, this is in stark contrast to the normal a-PET fluorescent sensors.[3,7] For **2**, fluorescence enhancement was observed by switching the pH from basic/neutral to acidic pH, and this is the typical a-PET effect.

The photophysical properties of the new sensors are significant. The fluorescence modulation efficiency of d-PET was greatly improved when compared to the reported d-PET sensors. For example, the fluorescence emission intensity of **1** shows 10-fold variation when the pH is switched from acidic to basic pH. For the reported analogue d-PET sensor (**4**), the enhancement is only 3-fold.[38] We noticed the lower signal modulation efficiency of 3-fold for **3**. However, compared to the ca. 0.25-fold emission intensity variation efficiency of the analogue with substitution at 3,6-position of the carbazole core (**6**, Scheme 1),[37] the signal modulation efficiency of **3**, which shows 3-fold emission enhancement upon switching the pH, is also greatly improved compared to its analogue **6**. The signal transduction of **3** is also higher than that of the reported **5** (1.5-fold). We propose that the greatly improved fluorescence signal modulation efficiency of the new sensors is due to the correct alignment of the electron donor (the carbazole moiety) and the electron acceptor group (the alkyl amine/boronic acid), i.e., the dipole moment and the transition moment of the sensor share the same direction; thus the electron transfer is significantly enhanced.

2.3. Orientation of the Dipole Moment and the Transition Moment of the Sensors: Influence on the Fluorescence Modulation Efficiencies of the d-PET Effect. We propose the alignment of the electron donor/acceptor of the sensors, either for the neutral form or the protonated form, significantly affect the fluorescence transduction efficiency of PET, which is vectorial electron transfer.[75] The orientation of the

(73) Lakowicz, J. R. *Principles of Fluorescence Spectroscopy*, 2nd ed.; Kluwer Academic: New York, 1999.
(74) Valeur, B. *Molecular fluorescence: principles and Applications*; Wiley-VCH Verlag GmbH: New York, 2001.
(75) Kumar, R. J.; Karlsson, S.; Streich, D.; Jensen, A. R.; Jäger, M.; Becker, H.-C.; Bergquist, J.; Johansson, O.; Hammarström, L. *Chem.—Eur. J.* **2010**, *16*, 2830–2842.

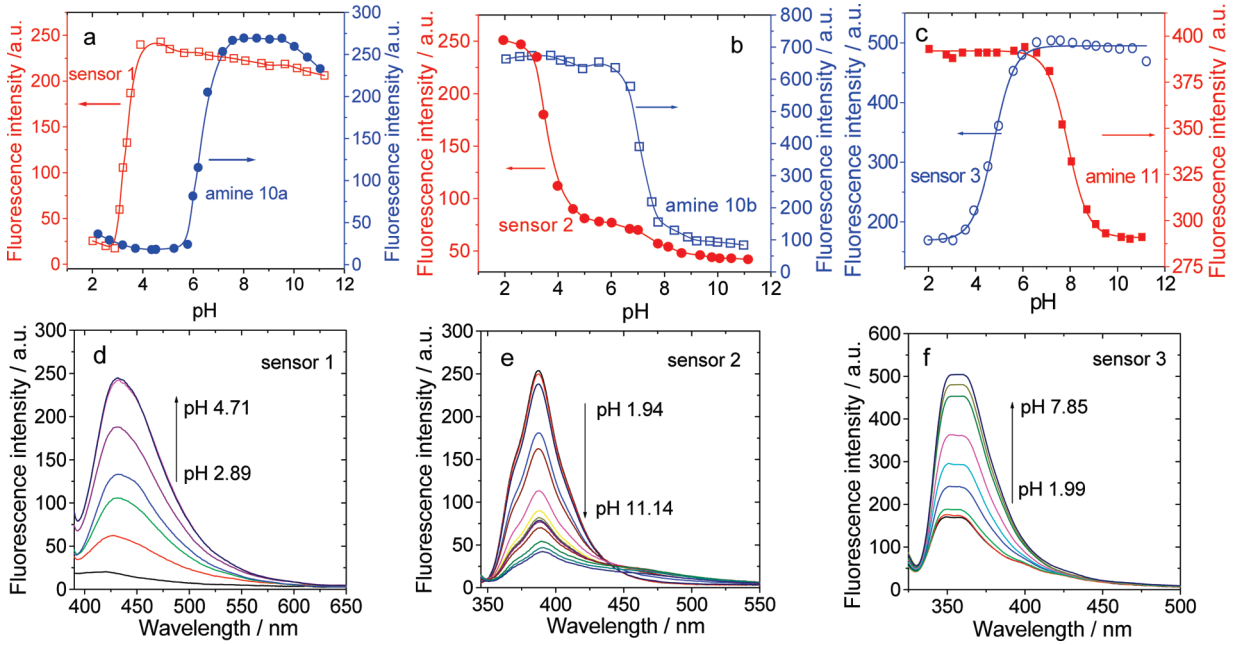

FIGURE 2. Fluorescence emission intensity−pH profile of the sensors and the amines: (a) Sensor **1** and amine **10a**: 3.0×10^{-6} mol dm^{-3} of **10a** (λ_{ex} 380 nm, λ_{em} 440 nm) and 1.0×10^{-6} mol dm^{-3} of sensor **1** (λ_{ex} 370 nm, λ_{em} 435 nm). (b) Amine **10b** and sensor **2**: 3.0×10^{-6} mol dm^{-3} of **10b** (λ_{ex} 330 nm, λ_{em} 388 nm and 1.0×10^{-6} mol dm^{-3} of **2** (λ_{ex} 335 nm, λ_{em} 390 nm). (c) Amine **11** and sensor **3**: 3.0×10^{-6} mol dm^{-3} of **11** (λ_{ex} 310 nm, λ_{em} 356 nm) and 1.25×10^{-6} mol dm^{-3} of **3** (λ_{ex} 315 nm, λ_{em} 356 nm). In 5.0×10^{-2} mol dm^{-3} NaCl ionic buffer (52.1% methanol in water). In order to compare the relative emission intensities of the sensors and the precursor amines, the emission spectra were not normalized. Emission spectra of the sensors (d) **1** (1.0×10^{-6} mol dm^{-3}), λ_{ex} 370 nm; (e) **2** (1.0×10^{-6} mol dm^{-3}), λ_{ex} 335 nm; (f) **3** (1.25×10^{-6} mol dm^{-3}), λ_{ex} 315 nm. Sensors in 5.0×10^{-2} mol dm^{-3} NaCl ionic buffer (52.1% methanol in water, w/w). 25 °C.

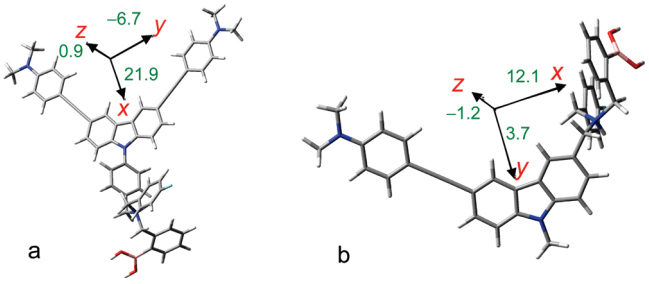

FIGURE 3. Dipole moment of the protonated (a) sensor **1** and (b) the sensor **4**. The dipole moment values at the *x*, *y*, and the *z* direction of the Cartesian axes are marked on the arrows. The Cartesian axes are read from the optimized structures. The dipole moment values are the optimization result of the protonated sensors. The direction of the electron transfer in both sensors is approximated as the *x* direction.

electron donor/acceptor of the sensors can be qualitatively evaluated by the dipole moment values. High dipole moments at the electron-transfer direction (transition moment direction) indicate that the orientation of the electron donor/acceptor is more ideal for the electron-transfer process to occur, whereas small dipole moment at the electron-transfer direction will result in poor electron transfer and thus low fluorescence modulation efficiency.

We compared the dipole moments of the neutral form of the sensor **1** with the analogue sensor **4**.[38] Using DFT calculations, the dipole moment of **1** was calculated as 3.8 D. This value is much higher than that of the analogue, i.e., **4**,[38] with a dipole moment of 2.1 D. We also compared the dipole moment at the electron-transfer direction (here it is the *x* direction in the Cartesian axes of the sensors). For neutral **1**, the dipole moment at the *x* direction is −2.1 D vs a small value of −0.8 D for neutral **4**.

The dipole moments of the protonated sensors **1** and **4** were compared (Figure 3). A large dipole moment of 22.9 D was observed for protonated sensor **1** vs a much smaller dipole moment of 12.5 D for protonated **4**.[38] The dipole moments at the electron-transfer direction, here it is also the *x* direction in the Cartesian axes of the sensors, are 21.9 and 12.1 D for protonated **1** and **4**, respectively. Thus, we conclude that the alignment of the electron donor/acceptor in **1** is more ideal for electron transfer than that of **4**. Indeed, we observed a much higher fluorescence transduction efficiency for **1** (10-fold emission intensity variation) compared to that of **4** (3-fold of emission intensity variation).

Similar results were observed for sensor **3**. Dipole moments of 5.3 and 11.7 D were determined for the neutral and protonated form of **3**, respectively. For its analogue **5**, however, dipole moment values of 3.3 and 5.4 D were observed, respectively.[37] More intuitive information can be obtained from the dipole moment of the protonated sensors in the electron transfer direction, which indicates that **3** shows much higher dipole moments at the electron transfer direction (−10.5 D) than protonated **5** (5.4 D). It should be pointed out that the distance between the fluorophore and the nonconjugated N-atom (switch of the fluorescence) of **3** is much larger than that of **5**, which probably diminishes the signal transduction efficiency of the PET effect.[7] However, we still observed high fluorescence transduction efficiency for **3** than that of **5**. This result infers that the dipole moment could play a significant role in the facilitation of the d-PET effect. Thus, the analogues demonstrated that higher dipole moment will result in higher fluorescence modulation efficiency.

TABLE 1. Photophysical Parameters of Sensors 1−3

sensors	ε^a (M^{-1} cm^{-1})	λ_{abs} (nm)	λ_{em} (nm)	Stokes shift/(nm)	Φ^b pH 3.0	Φ^b pH 6.0	τ^c (ns) pH 3.0	τ^c (ns) pH 6.0	$k_r{}^d$ pH 3.0	$k_r{}^d$ pH 6.0	$k_{nr}{}^e$ pH 3.0	$k_{nr}{}^e$ pH 6.0
1	1.44×10^4	372	435	63	0.001	0.031	4.72	1.25	0.21	2.48	21.2	77.5
2	2.72×10^4	343	390	47	0.15	0.047	1.36	8.12	11.0	0.58	62.5	11.7
3	1.67×10^4	345	356	11	0.06	0.46	8.23	6.52	0.73	7.05	11.2	8.28

[a]In 5.0×10^{-2} mol dm^{-3} NaCl ionic buffer (52.1% methanol in water), pH 7.5. [b]Fluorescence quantum yields, with quinine sulfate as the standard ($\Phi = 0.54$ in 0.5 M H_2SO_4). The estimated measuring error is 10%. [c]Fluorescence lifetimes, with typical error of 0.01 ns. Concentrations of the sensors are 1.0×10^{-5} mol dm^{-3}. [d]Radiative decay rate constants at pH 7.5, $k_r = \Phi/\tau$ ($\times 10^7$ s^{-1}). [e]Nonradiative decay rate constants at pH 7.5, $k_{nr} = (1-\Phi)/\tau$ ($\times 10^7$ s^{-1}).

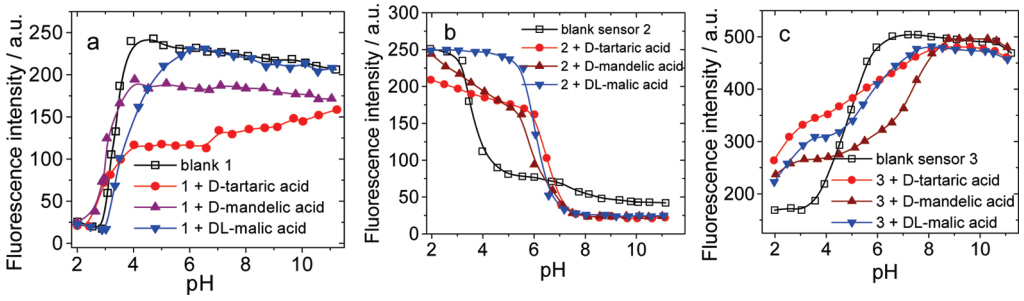

FIGURE 4. Emission intensity−pH profiles of the sensors in the presence of analytes of D-tartaric acid, D-mandelic acid, malic acid. (a) **1**: λ_{ex} 370 nm, λ_{em} 435 nm, 1.0×10^{-6} mol dm^{-3} of sensor. (b) **2**: 1.0×10^{-6} mol dm^{-3} of sensor **2**, λ_{ex} 335 nm, λ_{em} 390 nm. (c) Sensor **3**: 1.25×10^{-6} mol dm^{-3} of **3**, λ_{ex} 315 nm, λ_{em} 356 nm. The concentration of hydroxyl acids is 2.5×10^{-2} mol dm^{-3}, 5.0×10^{-2} mol dm^{-3} NaCl ionic buffer (52.1% methanol in water), 25 °C.

We also compared the dipole moment of the protonated forms of sensor **5** and **6**. We found that fluorescence transduction efficiency of **5** is higher than that of **6**.[37] Dipole moment values of 5.4 and 3.0 D were found for **5** and **6**, respectively. Thus, the fluorescence transduction efficiency of **5** and **6** can be rationalized by the dipole moments values. Furthermore, protonated **3** shows much higher dipole moment (−10.5 D) than that of **6** (3.0 D); thus, the higher fluorescence modulation efficiency of sensor **3** can be rationalized. The aforementioned higher fluorescence modulation efficiency for the 9-substituted sensors is in agreement with the observation that electron transfer is more efficient when an electron-accepting group is linked to *N*-atom (9-position) in carbazoles.[76,77] These findings may prove useful for the future design of efficient PET fluorescence sensors.

The photophysical properties of the sensors were compiled in Table 1. We observed a small Stokes shift for sensor **3**, which is similar to the carbazole and the **5**.[37] For **1** and **2**, however, the Stokes shifts are much larger. We measured the fluorescence quantum yields of the sensors at different pH. For the d-PET sensors (**1** and **3**), larger quantum yields were found at pH 6.0 than that at pH 3.0. For the a-PET **2**, however, larger quantum yield was observed at acidic pH.

2.4. pH Titration of the Sensors in the Presence of α-Hydroxyl Carboxylic Acids and the Binding Constants. The pH titration of the sensors in the presence of several typical analytes, such as α-hydroxyl carboxylic acids including tartaric acid, mandelic acid, and malic acid, were studied (Figure 4). For **1**, minor fluorescence enhancement was observed in the presence of analytes at pH 3.0. Instead emission diminishment was observed in the presence of analytes at neutral and basic pH. For **3**, recognition of the tartaric acid, mandelic acid, and malic acid was achieved by fluorescence enhancement at acid pH (pH 2.0−4.0). At neutral pH, the emission intensity was diminished in the presence of analytes. Interestingly, the fluorescence response toward mandelic acid and tartaric acid at pH 5.0 is enhancement and diminishment, respectively. Such a fluorescence transduction profile for chemoselectivity is rarely reported.[38] Previously, we observed a similar recognition profile for a carbazole-based d-PET sensor[37] and a chiral BINOL-based boronic acid sensor.[39] A normal a-PET recognition profile was observed for sensor **2**.

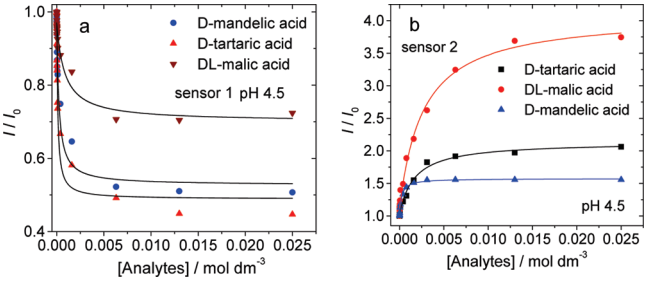

FIGURE 5. Binding isotherms of sensors with analytes. (a) Sensor **1** with hydroxyl acids, at pH 4.5: λ_{ex} = 370 nm, λ_{em} = 435 nm. (b) Sensor **2** with hydroxyl acids, at pH 4.5: λ_{ex} = 335 nm, λ_{em} = 389 nm. The solid lines are the fitting results of 1:1 binding. 1.0×10^{-6} mol dm^{-3} of sensor in 5.0×10^{-2} mol dm^{-3} NaCl ionic buffer (52.1% methanol in water). 25 °C.

The typical binding curves of the sensors **1** and **2** with α-hydroxyl carboxylic acids, such as tartaric acid, mandelic acid, and malic acid, were measured (Figure 5). pH 4.5 was selected to study the binding of **1** with the analytes. Fluorescence diminishment was observed in the presence of analytes. The binding of **1** with the analytes at pH 7.0 was also studied, and similar fluorescence diminishment was observed (see the Supporting Information). Different binding constants were observed for the interaction of the sensor with different analytes (Table 2).

(76) Adhikari, R. M.; Neckers, D. C.; Shah, B. K. *J. Org. Chem.* **2009**, *74*, 3341–3349.
(77) Kapturkiewicz, A.; Herbich, J.; Nowacki, J. K. *J. Phys. Chem. A* **1997**, *101*, 2332–2344.

TABLE 2. Stability Constants (M^{-1}) of Sensors 1−3 with α-hydroxyl Acids[a]

analytes	sensor **1**	sensor **2**	sensor **3**
Tartaric acid	$(9.04 \pm 1.95) \times 10^3$ pH 4.5 (↓)[b]	$(5.89 \pm 0.75) \times 10^2$ pH 4.5 (↑)	$(9.61 \pm 0.49) \times 10^2$ pH 3.0 (↑)[b]
	$(3.53 \pm 0.65) \times 10^3$ pH 7.0 (↓)	*c*	$(1.14 \pm 0.35) \times 10^4$ pH 5.0 (↑)
	c	*c*	$(1.07 \pm 0.21) \times 10^3$ pH 6.5 (↓)
Mandelic acid	$(4.29 \pm 1.04) \times 10^3$ pH 4.5 (↓)	$(4.34 \pm 0.36) \times 10^3$ pH 4.5 (↑)	$(1.31 \pm 0.11) \times 10^3$ pH 3.0 (↑)
	$(1.31 \pm 0.47) \times 10^3$ pH 7.0 (↓)	*c*	$(1.26 \pm 0.28) \times 10^5$ pH 5.0 (↓)
	c	*c*	$(6.57 \pm 0.83) \times 10^2$ pH 6.5 (↓)
malic acid	$(1.18 \pm 0.42) \times 10^3$ pH 4.5 (↓)	$(3.76 \pm 0.44) \times 10^2$ pH 4.5 (↑)	$(1.65 \pm 0.24) \times 10^3$ pH 3.0 (↑)
	$(5.96 \pm 1.63) \times 10^2$ pH7.0 (↓)	*c*	$(1.42 \pm 0.22) \times 10^4$ pH 6.5 (↓)

[a]Fluorescence intensity enhancement/diminishment in the presence of analytes is indicated in parentheses after the binding constants. [b]Fluorescence enhancement (↑) or diminishment (↓) in the presence of analytes is indicated. [c]Not determined.

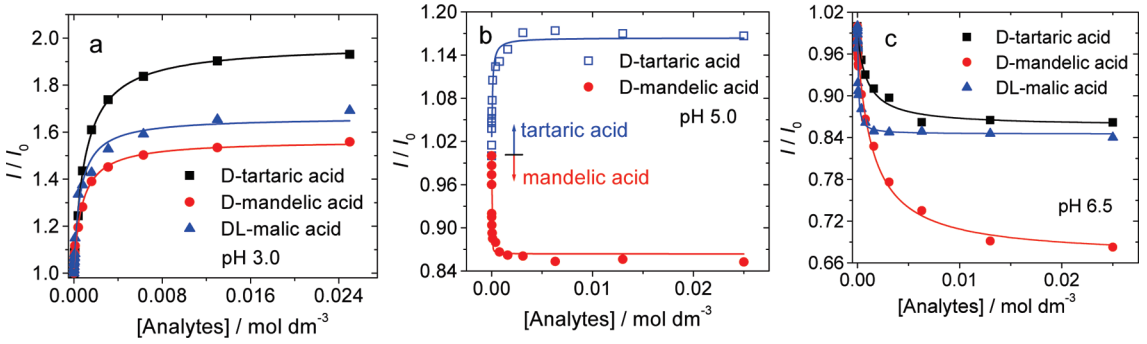

FIGURE 6. Binding curves of sensor **3** with α-hydroxyl carboxylic acids of tartaric acid, mandelic acid, and malic acid: λ_{ex} 315 nm, λ_{em} 356 nm. At pH 3.0, 5.0, and 6.5. The solid lines are the fitting results of 1:1 binding: λ_{ex} 315 nm, λ_{em} 356 nm. The estimated measuring error is 5%. 1.25×10^{-6} mol dm^{-3} of sensor in 5.0×10^{-2} mol dm^{-3} NaCl ionic buffer (52.1% methanol in water). 25 °C.

The binding of **3** with analytes was also studied. Fluorescence enhancement was observed in the presence of analytes at pH 3.0 (Figure 6). At pH 5.0, however, fluorescence enhancement and diminishment was observed in the presence of tartaric acid and mandelic acid, respectively. We propose that this sensing profile is due to the different apparent pK_a values of the sensor in the presence of the tartaric acid or mandelic acid (Figure 4).

The binding constants of the sensors with the analytes were compiled in Table 2. Chemoselectivity was observed for the d-PET sensors **1** and **3**, as well as the a-PET sensor **2**.

2.5. Rationalization of the d-PET Effect with the DFT/TDDFT Calculations. Recently, we found that the photophysical properties of lumophores can be studied using theoretical calculations, based on density functional theory (DFT) and the time-dependent DFT (TDDFT).[32,37,38] As a preliminary exploration, the geometry and the electronic structures of the excited state of sensor **1** were also studied in order to rationalize the d-PET effect.

The ground-state geometry of **1** was optimized (Figure 7). We found the dimethylamino phenylethynyl takes a coplanar geometry with the carbazole core; therefore, we propose an efficient π-conjugation effect between the arylethynyl appendents and the carbazole core. However, the phenyl group attached to the *N*-atom of the carbazole, through which the aryl boronic acid moiety is attached to the carbazole core, is tilted ca. 56° to the carbazole plan.[78] Thus, we do not expect efficient π-conjugation of this fragment with the carbazole core.[78] This is consistent with the experimental observations; for example, substitution at the *N*-position of the carbazole core does not perturb the photophysical properties of the carbazole core, such as the UV−vis absorption and fluorescence emission spectra (Figure 1).

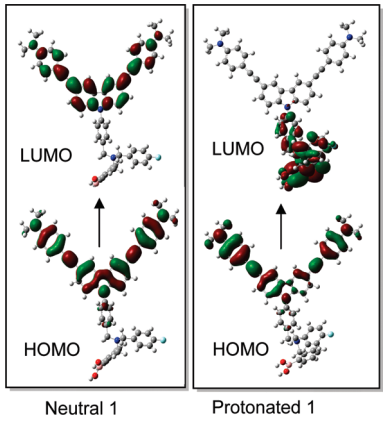

FIGURE 7. Frontier molecular orbits of neutral and protonated sensor **1**. Note the HOMO→LUMO transition of the neutral **1** is localized on the conjugated carbazole unit, whereas the HOMO→LUMO transition of protonated **1** is an electron-transfer process (π-conjugated carbazole→amine/boronic acid fragment). Calculated with the DFT/TDDFT methods based on the ground-state geometry of the neutral or the protonated form of the sensors on the B3LYP/6-31g(d) level.

In order to investigate the photophysical properties of the **1**, we investigated the excited-state electronic structure of the complex with the TDDFT methods (Table 3). For the neutral sensor **1**, a fully allowed $S_0 \rightarrow S_1$ transition was found (with excitation energy of 367 nm, oscillator strength f = 1.12). This is in full agreement with the UV−vis absorption band at 372 nm (Figure 1). The main frontier MOs are presented in Figure 7. By examining the molecular orbitals

(78) Ning, Z.; Chen, Z.; Zhang, Q.; Yan, Y.; Qian, S.; Cao, Y.; Tian, H. *Adv. Funct. Mater.* **2007**, *17*, 3799–3807.

TABLE 3. Selected Electronic Excitation Energies (eV) and Oscillator Strengths (*f*) and Configurations of the Low-Lying Excited States of the Neutral Sensor 1 and the Protonated Sensor 1 ($[1 + H]^+$) (Calculated by TDDFT//B3LYP/6-31G(d), Based on the Optimized Ground-State Geometries)

		TDDFT//B3LYP/6-31G(d)			
	electronic transitions	energy[a] (eV)	*f*[b]	composition[c]	CI[d]
1	$S_0 \rightarrow S_1$	3.37 (367 nm)	1.13	H→L	0.67
	$S_0 \rightarrow S_3$	3.51 (353 nm)	0.42	H−1→L+1	0.61
				H−1→ L+2	0.31
	$S_0 \rightarrow S_9$	4.01 (309 nm)	0.47	L→ L+5	0.56
				L→ L+6	0.24
$[\mathbf{1}+\mathbf{H}]^+$	$S_0 \rightarrow S_1$	1.84 (674 nm)	0.05	H→L	0.70
	$S_0 \rightarrow S_{18}$	3.28 (377 nm)	1.13	H→L+7	0.67

[a]Only selected excited states were considered. The numbers in parentheses are the excitation energy in wavelength. [b]Oscillator strength. [c]H stands for HOMO and L stands for LUMO. Only the main configurations are presented. [d]The CI coefficients are in absolute values.

involved in the $S_0 \rightarrow S_1$ transition, we found the HOMO and LUMO of neutral **1** show significant overlap. The large *f* value and the significant overlap of the MOs involved in the transition infers that the S_1 state of neutral **1** may be probably be an emissive state, which infers that the neutral compound is probably fluorescent.[38,79−81] $S_0 \rightarrow S_9$ transition was found with an excitation energy of 309 nm. These values are in good agreement with the UV−vis absorption spectra of sensor **1**.

For protonated **1**, however, the $S_0 \rightarrow S_1$ transition was found with an excitation energy of 674 nm and a small oscillator strength of 0.0541. No absorption at ca. 674 nm was found in the UV−vis absorption spectra (see the Supporting Information). Furthermore, we found the transition of HOMO→LUMO, which is the sole transition of the S_1 state, is a full electron-transfer process (from the dimethylaminophenylethynyl fragment to the protonated amine/boronic acid fragment); thus, there is no overlap between the HOMO and the LUMO. These results indicate that the S_1 state is a dark state and that protonated **1** is probably nonfluorescent.[38,79−81] These theoretical observations were completely validated by the experimental results. Thus, the d-PET effect of sensor **1** can be explained by the DFT/TDDFT calculations.

2.6. Conclusions. In conclusion, we have synthesized three new carbazole-based boronic acid sensors **1**−**3** to investigate the fluorescence modulation efficiency of the novel d-PET effect. The structural motifs of the sensors are fundamentally different from the previous d-PET sensors reported by us, in the alignment of the electron donor/acceptor and the distance between the nonconjugated *N* atom (as the fluorescence switch) and the fluorophore. Sensors **1** and **3** display a d-PET effect; i.e., these two sensors show diminished fluorescence emission at acidic pH but intensified emission at neutral/basic pH. Conversely, sensor **2** is an a-PET sensor, which shows intensified emission at acidic pH but diminished emission at neutral/basic pH. The fluorescence modulation efficiency of the d-PET effect for the new sensors, e.g., the emission intensity enhancement upon switching from acid pH to neutral pH, is up to 10-fold, which is a significant improvement from the previous d-PET sensors (ca. 3-fold of enhancement). We propose that the enhancement of the signal transduction efficiency of the new sensors is due to the correct orientation of the electron donor/acceptor of the sensors; i.e., the dipole moment and the transition moment of the sensor (photoinduced charge transfer transition) are oriented in the same direction, and thus, the PET process is facilitated. This is different from the previous d-PET sensors (with smaller dipole moment values and lower fluorescence transduction efficiency). Our results clearly indicate that a higher dipole moment along the vectorial direction of the PET effect results in higher fluorescence transduction efficiency for the sensor analogues. DFT/TDDFT calculations indicate a dark state S_1 for the protonated sensor **1** and an emissive state S_1 for the neutral sensor **1**; i.e., the neutral form may give much stronger emission than the protonated form, which is in agreement with the experimental observations. Selective recognition of tartaric acid, mandelic acid was achieved with the d-PET sensors. The importance of the alignment of the electron donor/acceptor pairs on the fluorescence modulation efficiency of the d-PET effect will aid the future design of PET fluorescent chemosensors with improved fluorescence modulation efficiency. In particular, it will be possible to optimize the transduction of PET sensors to achieve true OFF-ON modulation and hence dramatically enhanced sensitivity.

3. Experimental Section

3.1. Synthesis of 4-(9*H*-Carbazol-9-yl)benzaldehyde (7). 4-Fluorobenzaldehyde (12.5 g, 0.10 mol), carbazole (33.0 g, 0.20 mol), hexadecyltrimethylammonium bromide (0.5 g, 1.4 mmol), and K_2CO_3 (41.5 g, 0.30 mol) were mixed in DMSO (125 mL), and the mixture was heated at 100 °C for 72 h. The reaction mixture was cooled and poured into cold water. The mixture was extracted with dichloromethane (DCM). The organic layer was washed with water and dried over anhydrous Na_2SO_4. The solvent was removed under reduced pressure, and the residue was purified by column chromatography (silica gel, dichloromethane/petroleum ether = 1:3, V/V): 9.5 g of yellow powder; yield 35.0%; ^{1}H NMR (400 MHz, $CDCl_3$) δ 10.12 (s, 1H), 8.12−8.16 (m, 4H), 7.78 (d, 2H, J = 8.0 Hz), 7.49 (d, 2H, J = 8.0 Hz), 7.44 (t, 2H, J = 7.2 Hz), 7.33 (t, 2H, J = 7.2 Hz); ESI-HRMS ($C_{19}H_{13}NO^+$) calcd 271.0997, found 271.1004.

3.2. Synthesis of 4-(3,6-Diiodo-9*H*-carbazol-9-yl)benzaldehyde (8). 4-(3,6-Diiodo-9*H*-carbazol-9-yl)benzaldehyde was synthesized according to a literature procedure.[82]

3.3. Synthesis of 4-[3,6-Bis[[4-(dimethylamino)phenyl]ethynyl]-9*H*-carbazol-9-yl]benzaldehyde (9a). Under an argon atmosphere, 4-(3,6-diiodo-9*H*-carbazol-9-yl)benzaldehyde (0.8 g, 1.53 mmol) and $Pd(PPh_3)_4$ (170 mg, 0.15 mmol) were dissolved in triethylamine (20 mL). 4-Ethynyl-*N*,*N*-dimethylaniline (507 mg, 3.5 mmol) was added to the above solution followed by addition of CuI (41.7 mg, 0.22 mmol). The mixture was stirred at 60 °C for 8 h. After removal of triethylamine under reduced pressure, the residue was purified by column chromatography (silica gel; dichloromethane/petroleum ether = 2:1, v/v) to give 280 mg of a yellow solid: yield 33.0%; mp > 300 °C; ^{1}H NMR (400 MHz, $CDCl_3$) δ 10.13 (s, 1H), 8.28 (s, 2H), 8.15 (d, 2H, J = 8.0 Hz), 7.78 (d, 2H, J = 8.4 Hz), 7.58 (d, 2H, J = 8.4 Hz), 7.46 (d, 4H, J = 8.8 Hz), 7.41 (d, 2H, J = 8.4 Hz), 6.71 (d, 4H, J = 6.4 Hz), 3.01 (s, 12H);

(79) Saita, K.; Nakazono, M.; Zaitsu, K.; Nanbu, S.; Sekiya, H. *J. Phys. Chem. A* **2009**, *113*, 8213–8220.
(80) Zhao, G.; Liu, J.; Zhou, L.; Han, K. *J. Phys. Chem. B* **2007**, *111*, 8940–8945.
(81) Matsika., S. *J. Phys. Chem. A* **2004**, *108*, 7584–7590.
(82) Xu, T.; Lu, R.; Liu, X.; Chen, P.; Qiu, X.; Zhao, Y. *Eur. J. Org. Chem.* **2008**, 1065–1071.

^{13}C NMR (100 MHz, $CDCl_3$) δ 190.9, 150.2, 142.9, 139.8, 135.2, 132.8, 131.6, 130.1, 127.0, 123.9, 117.1, 112.1, 110.6, 110.0, 94.6, 89.7, 88.0, 40.4; ESI-MS ($[C_{39}H_{31}N_3O + H]^+$) calcd 558.2545, found 558.2549.

3.4. Synthesis of 3,6-Bis[[4-(dimethylamino)phenyl]ethynyl]-9-[4-[(4-fluorobenzyl)aminomethyl]phenyl]-9*H*-carbazole (10a). Compound **9a** (150 mg, 0.27 mmol) and 4-fluorobenzylamine (50 mg, 0.40 mmol) were dissolved in ethanol/THF (3:2, v/v). The mixture was refluxed with stirring for 6 h under N_2. The solvent was removed under reduced pressure, the residue was dissolved in 10 mL of MeOH/THF, $NaBH_4$ (25 mg, 0.66 mmol) was added in several portions, and the mixture was stirred for 15 min at room temperature. The solvent was removed, and the residue was taken up with DCM, the organic phase was washed with brine and dried over Na_2SO_4, DCM was removed, and the residue was purified by column chromatography (silica gel, DCM/MeOH, 100:1, v/v). A light yellow oil was obtained in quantitative yield: ^{1}H NMR (400 MHz, $CDCl_3$) δ 8.27 (s, 2H), 7.60 (d, 2H, J = 8.0 Hz), 7.54 (d, 2H, J = 8.4 Hz), 7.50 (d, 2H, J = 8.4 Hz), 7.45 (d, 4H, J = 8.8 Hz), 7.39 (d, 2H, J = 8.0 Hz), 7.30 (d, 2H, J = 8.4 Hz), 7.03−7.08 (m, 2H), 6.68 (d, 4H, J = 8.8 Hz), 3.94 (s, 2H), 3.90 (s, 2H) 3.00 (s, 12H); ESI-HRMS ($[C_{46}H_{39}FN_4 + H]^+$) calcd 667.3237, found 667.3264.

3.5. Synthesis of 2-[[[[4-[3,6-Bis[[4-(dimethylamino)phenyl]-ethynyl]-9*H*-carbazol-9-yl]]phenylmethyl](4-fluorobenzyl)amino]-methyl]phenylboronic Acid (1). Compound **10a** (67 mg, 0.10 mmol), 2-(2-bromomethylphenyl)-1,3,2-dioxaborinane (40 mg, 0.16 mmol), and K_2CO_3 (60 mg, 0.43 mmol) were mixed in DCM (5 mL), and the mixture was stirred at room temperature for 12 h under N_2. Then 10 mL of DCM was added. The organic layer was washed with water and dried over anhydrous Na_2SO_4. The solvent was removed, and the residue was purified by column chromatography (Al_2O_3, DCM/MeOH, 30:1, v/v): 35.0 mg of yellow powder was obtained; yield 44.0%; mp 167.3−168.9 °C; ^{1}H NMR (400 MHz, $CDCl_3$/CD_3OD) δ 8.28 (s, 2H), 7.55 (d, 2H, J = 8.4 Hz), 7.45−7.47 (m, 8H), 7.29−7.35 (m, 8H), 7.03−7.07 (m, 2H), 6.70 (d, 4H, J = 8.0 Hz), 3.82 (s, 2H), 3.71 (s, 4H), 3.00 (s, 12H); ^{13}C NMR (100 MHz, $CDCl_3$/CD_3OD) δ 163.6, 161.2, 150.1, 141.2, 140.4, 136.4, 136.2, 132.7, 131.8, 131.7, 131.6, 131.3, 130.2, 129.8, 127.6, 126.8, 123.7, 123.1, 116.0, 115.6, 115.3, 112.2, 110.7, 110.0, 89.1, 88.2, 62.0, 57.3, 57.1; ESI-HRMS ($C_{53}H_{46}BFN_4O_2 + H^+$) calcd 801.3776, found 801.3803; ($[C_{54}H_{48}BFN_4O_2 + H]^+$) calcd 815.3933, found 815.3929.

3.6. Synthesis of [9-[4-[(4-Fluorobenzyl)aminomethyl]phenyl]]carbazole (11). Compound **7** (270 mg, 1.0 mmol) and 4-fluorobenzylamine (250 mg, 2.0 mmol) were dissolved in ethanol/THF (3:2, v/v). The mixture was refluxed with stirring for 6 h under N_2. The solvent was removed under reduced pressure, the residue was dissolved in 15 mL of MeOH/THF, $NaBH_4$ (78.0 mg, 2.0 mmol) was added in several portions, and the mixture was stirred for 15 min at room temperature. The solvent was removed, the residue was taken up with DCM, the organic phase was washed with brine and dried over Na_2SO_4, DCM was removed, and the residue was purified with column chromatography (silica gel, DCM/MeOH, 50:1, v/v). A light yellow oil was obtained in quantitative yield: ^{1}H NMR (400 MHz, $CDCl_3$) δ 8.11 (d, 2H, J = 8.0 Hz), 7.52 (d, 2H, J = 8.4 Hz), 7.47 (d, 2H, J = 8.4 Hz), 7.37 (d, 4H, J = 4.0 Hz), 7.33 (d, 1H, J = 5.6 Hz), 7.31 (d, 1H, J = 5.6 Hz), 7.27 (d, 1H, J = 4.0 Hz), 7.25 (d, 1H, J = 4.0 Hz), 6.99−7.02 (m, 2H), 3.87 (s, 2H), 3.82 (s, 2H); ^{13}C NMR (100 MHz, $CDCl_3$) δ 163.4, 160.9, 141.1, 139.7, 136.6, 129.7, 127.2, 126.0, 123.5, 120.4, 120.0, 115.5, 115.2, 109.9, 52.9, 52.8; ESI-MS ($[C_{26}H_{21}FN_2 + H]^+$) calcd 381.1767, found 381.1777.

3.7. Synthesis of 2-[[[4-(9*H*-Carbazol-9-yl)phenylmethyl](4-fluorobenzyl)amino]methyl]phenylboronic Acid (3). Compound **11** (95 mg, 0.25 mmol), 2-(2-bromomethylphenyl)-1,3,2-dioxaborinane (80 mg, 0.32 mmol), and K_2CO_3 (150 mg, 1.08 mmol) were mixed in dichloromethane (4 mL), and the mixture was stirred at room temperature for 12 h under N_2. Then 5 mL of DCM was added. The organic layer was washed with water and dried over anhydrous Na_2SO_4. The solvent was removed, and the residue was purified with column chromatography (Al_2O_3, DCM/MeOH, 100:1, V/V): 51.0 mg of yellow powder was obtained; yield 39.0%; mp 159.2−160.5 °C; ^{1}H NMR (400 MHz, $CDCl_3$/CD_3OD) δ 8.13 (d, 2H, J = 7.6 Hz), 7.38−7.42 (m, 4H), 7.33−7.36 (m, 4H), 7.25−7.32 (m, 3H), 7.03−7.08 (m, 2H), 3.80 (s, 2H), 3.72 (s, 2H), 3.70 (s, 2H); ^{13}C NMR (100 MHz, CD_3OD) δ 164.9, 162.5, 142.4, 142.2, 138.3, 137.7, 134.2, 132.8, 132.7, 132.5, 129.5, 128.0, 127.9, 127.0, 124.7, 121.2, 121.1, 116.2, 115.9, 110.7, 57.8, 57.7, 54.8; ESI-HRMS ($[C_{33}H_{28}BFN_2O_2 + H]^+$) calcd 515.2306, found 515.2312; ($[C_{34}H_{30}BFN_2O_2 + H]^+$, adduct with one molecule of MeOH) calcd 529.2463, found 529.2446.

3.8. Synthesis of 4-[3,6-Bis(phenylethynyl)-9*H*-carbazol-9-yl]benzaldehyde (9b). Under an argon atmosphere, 4-(3,6-diiodo-9*H*-carbazol-9-yl)benzaldehyde (800 mg, 1.53 mmol) and $Pd(PPh_3)_4$ (170 mg, 0.15 mmol) were dissolved in 20 mL of triethylamine. Ethynylbenzene (380 mg, 3.7 mmol) was added to the above solution and followed by addition of CuI (41.7 mg, 0.22 mmol). The mixture was stirred at 60 °C for 8 h. After removal of triethylamine under reduced pressure, the residue was purified with column chromatography (silica gel; dichloromethane/Petroleum ether, 5:1, v/v) to give 403 mg of a yellow solid: yield 56.0%; mp 178.8−179.4 °C; ^{1}H NMR (400 MHz, $CDCl_3$) δ 10.12 (s, 1H), 8.32 (s, 2H), 8.14 (d, 2H, J = 8.4 Hz), 7.76 (d, 2H, J = 8.0 Hz), 7.57−7.63 (m, 6H), 7.42 (d, 2H, J = 8.4 Hz), 7.34−7.40 (m, 6H); ^{13}C NMR (100 MHz, $CDCl_3$) δ 191.0, 142.6, 140.2, 135.3, 131.7, 130.5, 128.6, 128.3, 127.1, 124.4, 123.7, 123.6, 116.2, 110.2, 94.6, 90.1, 88.7; MS ($[C_{35}H_{21}NO + H]^+$) calcd 472.16, found 472.20.

3.9. Synthesis of 3,6-Bis(phenylethynyl)-9-[4-[(4-fluorobenzyl)-aminomethyl]phenyl]-9*H*-carbazole (10b). Compound **9b** (150 mg, 0.32 mmol) and 4-fluorobenzylamine (80 mg, 0.64 mmol) were dissolved in ethanol/THF (7:2, v/v). The mixture was refluxed with stirring for 6 h under N_2. The solvent was removed under reduced pressure, the residue was dissolved in 10 mL of MeOH/THF, $NaBH_3CN$ (100 mg, 1.6 mmol) was added in several portions and the mixture was stirred for 15 min at room temperature. The solvent was removed, the residue was taken up with DCM, the organic phase was washed with brine and dried over Na_2SO_4, DCM was removed, and the residue was purified with column chromatography (silica gel, DCM/MeOH, 50:1, V/V). A light yellow oil was obtained in quantitative yield: ^{1}H NMR (400 MHz, $CDCl_3$) δ 8.33 (s, 2H), 7.59−7.61 (m, 8H), 7.50 (d, 2H, J = 8.0 Hz), 7.28−7.39 (m, 10H), 7.03−7.08 (m, 2H), 3.93 (s, 2H), 3.88 (s, 2H); ^{13}C NMR (100 MHz, $CDCl_3$) δ 163.7, 161.1, 141.1, 131.7, 130.6, 130.2, 130.0, 128.5, 128.1, 127.2, 124.3, 123.9, 123.2, 115.9, 115.6, 115.5, 115.3, 110.3, 90.6, 88.3, 54.8. 52.8; ESI-HRMS ($[C_{42}H_{29}FN_2 + H]^+$) calcd 581.2393, found 581.2370.

3.10. Synthesis of 2-[[[[4-[3,6-Bis(phenylethynyl)-9*H*-carbazol-9-yl]]phenylmethyl](4-fluorobenzyl) amino]methyl]phenylboronic Acid (2). Compound **10b** (100 mg, 0.17 mmol), 2-(2-bromomethylphenyl)-1,3,2-dioxaborinane (60.0 mg, 0.24 mmol), and K_2CO_3 (90.0 mg, 0.65 mmol) were mixed in dichloromethane (5 mL), and the mixture was stirred at room temperature for 12 h under N_2. Then 10 mL of dichloromethane was added. The organic layer was washed with water and dried over anhydrous Na_2SO_4. The solvent was removed and the residue was purified with column chromatography (Al_2O_3, DCM/MeOH, 50:1, v/v): 45 mg of yellow powder was obtained; yield 37.0%; mp 97.1−98.2 °C; ^{1}H NMR (400 MHz, $CDCl_3$/CD_3OD) δ 8.33 (s, 2H), 7.58−7.61 (m, 6H), 7.48 (s, 4H), 7.32−7.40 (m, 14H), 7.24 (d, 1H, J = 7.2 Hz), 7.04−7.08 (m, 2H), 3.83 (s, 2H), 3.72 (s, 4H); ^{13}C NMR (100 MHz, $CDCl_3$/CD_3OD) δ 163.7, 161.2,

141.2, 140.9, 136.6, 136.4,136.2, 131.8, 131.4, 131.3, 130.2, 129.0, 128.5, 128.1, 127.7, 127.0, 126.9, 124.2, 123.8, 123.1, 115.7, 115.4, 115.3, 110.2, 90.5, 88.3, 62.1, 57.5, 57.2; ESI-HRMS ($[C_{50}H_{38}BFN_2O_2 + H]^+$) calcd 729.3089, found 729.3062.

3.11. Computational Details. The ground state structures of sensors **1**−**3** were optimized using density functional theory (DFT) with B3LYP functional and 6-31G(d) basis set. The excited-state related calculations were carried out with the time-dependent DFT (TDDFT), based on the optimized structure of the ground state. There are no imaginary frequencies in frequency analysis of all calculated structures. All these calculations were performed with Gaussian 09.[83]

Acknowledgment. We thank the NSFC (20642003, 20634040, 40806042, and 20972024), Ministry of Education (SRF for ROCS, SRFDP-200801410004 and NCET-08-0077), PCSIRT (IRT0711), State Key Laboratory of Fine Chemicals (KF0710 and KF0802), State Key Laboratory of Chemo/Biosensing and Chemometrics (2008009), the Education Department of Liaoning Province (2009T015), and Dalian University of Technology (SFDUT07005, 1000-893394) for financial support. We are grateful for the support of the Royal Society (UK) through the China−UK Science Networks program. The support has helped initiate annual Symposia and Joint Laboratories devoted to Catalysis & Sensing for our Environment (CASE).

Supporting Information Available: General experimental methods, ^1H and ^{13}C NMR data of the compounds, photophysical data and solvent effect of the dyes, theoretical calculations details (**z**-matrix), and theoretical rationalization of the PET effect of the boronic acid sensors. This material is available free of charge via the Internet at http://pubs.acs.org.

(83) Frisch, M. J.; Trucks, H. W., et al. *Gaussian 09, Revision A. 1*; Gaussian, Inc.: Wallingford, CT, 2009.